ORIGINAL ARTICLE

WILEY **Cancer Science**

Molecular pathogenesis of pancreatic ductal adenocarcinoma: Impact of passenger strand of pre-*miR-148a* on gene regulation

Tetsuya Idichi[1] [iD] | Naohiko Seki[2] | Hiroshi Kurahara[1] [iD] | Haruhi Fukuhisa[1] |
Hiroko Toda[1] | Masataka Shimonosono[1] | Atsushi Okato[2] | Takayuki Arai[2] |
Yoshiaki Kita[1] | Yuko Mataki[1] | Yuko kijima[1] | Kosei Maemura[1] | Shoji Natsugoe[1]

[1]Department of Digestive Surgery, Breast and Thyroid Surgery, Graduate School of Medical Sciences, Kagoshima University, Kagoshima, Japan

[2]Department of Functional Genomics, Chiba University Graduate School of Medicine, Chiba, Japan

Correspondence
Naohiko Seki, Department of Functional Genomics, Chiba University Graduate School of Medicine, Chiba, Japan.
Email: naoseki@faculty.chiba-u.jp

We previously used RNA sequencing to establish the microRNA (miRNA) expression signature of pancreatic ductal adenocarcinoma (PDAC). We found that both strands of pre-*miR-148a* (*miR-148a-5p*: the passenger strand and *miR-148a-3p*: the guide strand) were downregulated in cancer tissues. Ectopic expression of *miR-148a-5p* and *miR-148a-3p* significantly inhibited cancer cell migration and invasion, indicating that both strands of pre-*miR-148a* had tumor-suppressive roles in PDAC cells. In silico database and genome-wide gene expression analyses identified a total of 15 genes that were putative targets regulated by these miRNAs. High expression of *miR-148a-5p* targets (*PHLDA2*, *LPCAT2* and *AP1S3*) and *miR-148a-3p* targets (*SMA*, *ENDOD1* and *UHMK1*) was associated with poor prognosis of patients with PDAC. Moreover, knockdown of *PHLDA2* expression inhibited cancer cell aggressiveness, suggesting *PHLDA2* acted as an oncogene in PDAC cells. Involvement of the passenger strand of pre-*miR-148a* (*miR-148-5p*) is a new concept in cancer research. Novel approaches that identify tumor-suppressive miRNA regulatory networks in lethal PDAC might provide new prognostic markers and therapeutic targets for this disease.

KEYWORDS
cancer genome/genetics, characteristics and pathology of human cancer, information, invasion and metastasis, oncogenes and tumor-suppressor genes

1 | INTRODUCTION

Pancreatic ductal adenocarcinoma (PDAC) is one of the most lethal cancers known to medicine. The 5-year survival period of patients with PDAC is approximately 5%.[1] At first diagnosis, most patients with PDAC have local invasion or distant metastasis, and only about 15% of patients are candidates for surgical resection.[2] Currently developed combination chemotherapies have a limited therapeutic impact on patients with advanced stage disease.[3] Therefore, improved understanding of the underlying pathological mechanisms could lead to new therapeutic approaches for this disease.

In recent years, microRNA (miRNA) has received considerable attention as a crucial molecule that controls the expression of protein-coding or non-coding genes. Regulation is achieved by translational repression or mRNA cleavage in a sequence-specific method.[4] Currently developed bioinformatics approaches indicate that 1 miRNA can regulate thousands of mRNAs and, conversely, most protein-coding genes in the genome are under the control of miRNAs.[5]

Therefore, aberrantly expressed miRNAs can disturb entire networks of mRNAs and proteins.

Identification of dysregulated miRNAs in cancer cells is an important first step in elucidating aberrantly expressed genes and proteins in cancer. Based on this background, our groups have been comprehensively studying specimens of several cancers by genome-wide miRNA expression analyses.[6,7] Analyses of miRNA expression signatures of PDAC clinical specimens by RNA sequencing showed that some passenger strands of miRNAs (eg, *miR-216a-3p, miR-216b-3p, miR-148a-5p, miR-129-1-3p* and *miR-129-2-3p*) were significantly downregulated in cancer tissues.[8] In miRNA biogenesis, it is generally believed that 1 strand of the mature duplex miRNA (the guide strand) is incorporated into the miRNA-induced silencing complex (RISC) and its control target genes by RNA degradation and translational repression.[9] In contrast to the guide strand, the passenger strand of miRNA was previously thought to be degraded and to have no function.[10,11]

Contrary to established beliefs, our recent studies indicated that several passenger strands of miRNAs acted as antitumor miRNAs in several cancers.[12,13] For example, *miR-145-3p* (passenger strand) was significantly downregulated in castration-resistant prostate cancer and restoration of *miR-145-3p* inhibited cancer cell migration and invasion through targeting of *MELK, NCAPG, BUB1*, and *CDK1*.[14] Similarly, antitumor functions have also been shown in bladder cancer and lung cancer.[15,16] Realization that the passenger strand of miRNA is involved in the regulation of RNA networks will improve our understanding of cancer cell development and tumor progression.

In the present study, our goal was to identify novel therapeutic targets in lethal PDAC. Based on our original miRNA expression signature of PDAC, we focused on pre-*miR-148a* (*miR-148a-5p* [passenger strand] and *miR-148a-3p* [guide strand]) and investigated the functional significance of these miRNAs and their regulatory RNA networks in PDAC cells. Elucidation of molecular networks modulated by novel antitumor miRNAs in PDAC cells may provide new insights into the pathological mechanisms underlying the disease.

2 | MATERIALS AND METHODS

2.1 | Clinical specimens and cell lines

Clinical tissue specimens (n = 30) were obtained from patients with PDAC who underwent curative surgical resection at Kagoshima University Hospital between 1997 and 2016. Normal pancreatic tissue specimens (n = 18) were obtained from non-cancerous tumor-adjacent tissues. Each surgical specimen was histologically characterized according to the TNM classification system.[17] All patients in this study provided informed consent and the study protocol was approved by the Institutional Review Board of Kagoshima University. Quantitative real-time PCR (qRT-PCR) of clinical samples was carried out by extracted total RNA from frozen specimens, immunohistochemistry was performed by PDAC tissues from formalin-fixed paraffin-embedded. Two human PDAC cell lines (PANC-1 and SW1990) were used in this study as described previously.[8,18,19]

2.2 | Quantitative real-time PCR

Protocols for total RNA extraction from clinical specimens and cell lines were described in previous studies. The procedure for quantification of miRNAs and mRNAs was described earlier.[18-21] TaqMan qRT-PCR probes and primers were obtained from Thermo Fisher Scientific (Waltham, MA, USA) as follows: *miR-148a-5p* (product ID: 002134); *miR-148a-3p* (product ID: 000470); *PHLDA2*(product ID: Hs00169368_m1); *LPCAT2* (product ID: Hs01044164_m1); *AP1S3* (product ID: Hs00950999_m1); *SMS* (product ID: Hs01924834_u1); *ENDOD1* (product ID: Hs00826684_m1); *UHMK1* (product ID: Hs00332674_m1). Human *GUSB* (product ID: Hs99999908_m1), *RNU48* (product ID: 001006), *miR-26a* (product ID: 000405), *miR-21* (product ID: 000397) were used as internal controls.

2.3 | Transfection of miRNA mimic, siRNA and cDNA cloning into PDAC cell lines

The procedure for miRNA, siRNA and cDNA plasmid transfection into cancer cells was described previously.[18-21] Pre-miR™ miRNA precursors for *miR-148a-5p* (product ID: PM 12683), *miR-148a-3p* (product ID: PM 10263), negative control miRNA (product ID: AM 17010), 2 *PHLDA2* siRNAs (product IDs: HSS144353 and HSS144354) and negative control siRNA (product ID: D-001810-10) were purchased from Thermo Fisher. A Flexi HaloTag cDNA clone of *PHLDA2* (Vector: pFN21A, Product ID: FHC02241) was purchased from Kazusa Genome Technologies (Chiba, Japan). Transfection efficiencies of miRNA and siRNA in cell lines were calculated as described.[22]

2.4 | Cell proliferation, migration and invasion assays

Protocols for functional assays (cell proliferation, migration and invasion) were described previously.[18-21]

2.5 | Argonaute 2(Ago2)-bound miRNA isolation by immunoprecipitation

PANC-1 and SW1990 cells growing on 6-well plates were transfected with 10 nmol/L pre-*miR-148a*. After reverse transfection, immunoprecipitation was carried out using a microRNA Isolation kit, Human Ago2 (Wako, Osaka, Japan). The procedure was as described previously.[13,14]

2.6 | Western blot analyses and immunohistochemistry

Antibodies against PHLDA2 (product ID: ab99209; Abcam, Tokyo, Japan), poly (ADP-ribose) polymerase (PARP) antibody (product ID: 9542; Cell Signaling Technology, Danvers, MA, USA) and GAPDH (product ID: SAF6698; Wako) were used in this study. The procedures for western blotting and tissue immunohistochemistry were as described previously.[18,19,23]

2.7 | Genome-wide gene expression and in silico analyses

To identify genes targeted by *miR-148a-5p* and *miR-148a-3p*, we used a combination of in silico analyses and genome-wide gene expression analyses as described previously.[18,19,23] Expression data by microarray analyses were deposited into the Gene Expression Omnibus (GEO) database (accession numbers GSE15471, GSE93290).

2.8 | The Cancer Genome Atlas (TCGA) database analysis of PDAC specimens

The clinical significance of the expression of miRNAs or target genes and relation to PDAC pathogenesis were determined with the OncoLnc database (http://www.oncolnc.org).[18,24,25] Clinical information on 174 PDAC samples was obtained from National Cancer Institute GDC Data Portal (https://portal.gdc.cancer.gov) and cBioPortal (http://www.cbioportal.org). TNM stage, T stage, N stage and M stage on TCGA pathological database were evaluated by The American Joint Committee on Cancer (AJCC). Disease-free survival (DFS) within 3 years and recurrence were analyzed in 113 PDAC samples where data were disclosed.

2.9 | Plasmid construction and dual-luciferase reporter assay

The vector used for dual-luciferase reporter assay was psiCHECK-2 vector (C8021; Promega, Madison, WI, USA). The cloned sequences are listed in Figure S1. The procedure for dual-luciferase reporter assay was described previously.[18-21]

2.10 | Identification of downstream targets regulated by *PHLDA2* in PDAC

Genome-wide microarray analysis was applied for identification of *PHLDA2* downstream targets. Expression data were deposited in the GEO database (GSE106791). Genes downregulated by *PHLDA2* were assessed for PDAC prognosis using TCGA database.

2.11 | Statistical analysis

Relationships between 2 groups and expression values obtained by qRT-PCR were analyzed using the Mann-Whitney *U* test. Correlation between expression of *miR-148a-5p*, *miR-148a-3p* and *PHLDA2* was evaluated using Spearman's rank test. Relationships among more than 3 variables and numerical values were analyzed using the Bonferroni-adjusted Mann-Whitney *U* test. Overall survival (OS) and DFS after surgery were gauged using Kaplan–Meier curves. Patients were divided into 2 groups based on high and low gene expression around the median, and differences in survival were estimated using the log-rank test. We used Expert StatView software (version 5.0; SAS Institute Inc., Cary, NC, USA) for these analyses.[18,19]

3 | RESULTS

3.1 | Expression levels of *miR-148a-5p* and *miR-148a-3p* in PDAC specimens and cell lines
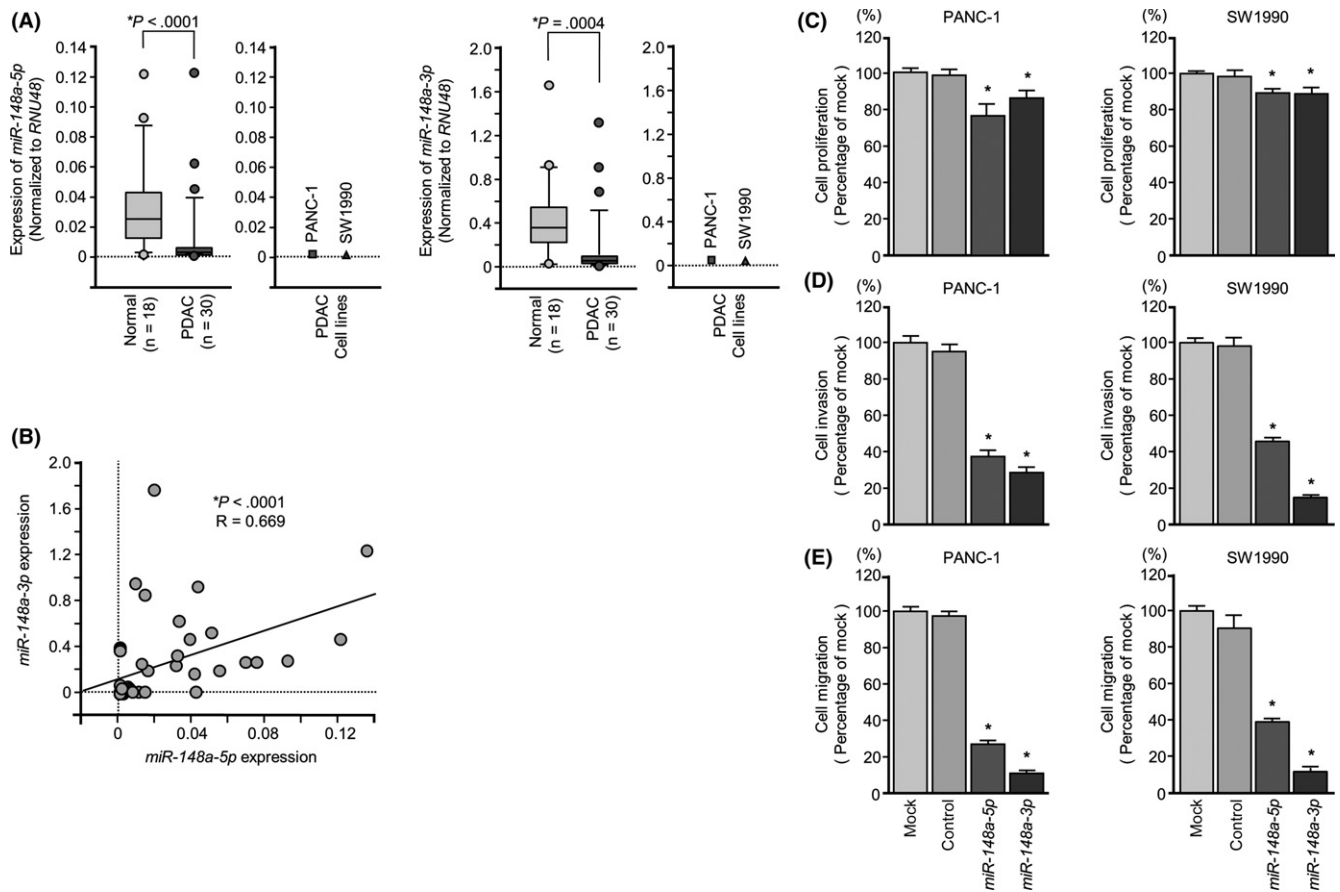
Expression levels of *miR-148a-5p* and *miR-148a-3p* in PDAC tissues (n = 30), normal pancreatic tissues (n = 18) and 2 PDAC cell lines (PANC-1 and SW1990) were evaluated. Characteristics of the clinical samples are summarized in Tables 1,2 . Expression levels of *miR-148a-5p* and *miR-148a-3p* were significantly lower in tumor tissues compared with normal pancreatic tissues ($P < .0001$ and $P = .0004$, respectively, Figure 1A). Spearman's rank test showed positive correlations between the expression of *miR-148a-5p* and *miR-148a-3p* ($R = .669$ and $P < .0001$; Figure 1B). However, there were no significant relationships between any of the clinical features

TABLE 1 Characteristics of patients in the present study: pancreatic ductal adenocarcinoma

Total no.	30
Average age (range) years	65.4 (42-85)
Gender (%)	
Male	14 (46.7)
Female	16 (53.3)
T category (%)	
pTis	1 (3.3)
pT1	10 (33.3)
pT2	13 (43.3)
pT3	4 (13.3)
pT4	2 (6.7)
N category (%)	
0	17 (56.7)
1	13 (43.3)
M category (%)	
0	28 (93.3)
1	2 (6.7)
Neoadjuvant chemotherapy (%)	
(−)	12 (40.0)
(+)	18 (60.0)
Recurrence (%)	
(−)	13 (43.3)
(+)	17 (56.7)

TABLE 2 Characteristics of patients in the present study: normal pancreatic tissue

Total no.	18
Average age (range) years	65.9 (42-85)
Gender (%)	
Male	7 (38.9)
Female	11 (61.1)

FIGURE 1 Antitumor functions of *pre-miR-148a* in pancreatic ductal adenocarcinoma (PDAC) cell lines (PANC-1 and SW1990). A, Expression levels of *miR-148a-5p and miR-148a-3p* in PDAC clinical specimens and cell lines were determined by qRT-PCR. Data were normalized to *RNU48* expression. B, Expression levels of *miR-148a-3p* and *miR-148-5p* were positively correlated ($R = .699$, $P < .0001$). C, Cell proliferation was determined by XTT assays 72 h after transfection with 10 nmol/L *miR-148a-5p* or *miR-148a-3p*, *$P < .0001$. D, Cell invasion activity was determined using Matrigel invasion assays, *$P < .0001$. E, Cell migration activity was determined by migration assays, *$P < .0001$

(ie, neoadjuvant chemotherapy, metastasis or recurrence) and the expression of *miR-148a-5p* and *miR-148a-3p* (data not shown).

3.2 | Both *miR-148a-5p* and *miR-148a-3p* bound to Ago2

To investigate whether the *miR-148a-5p* (passenger strand) is incorporated into RISC, we carried out immunoprecipitation with antibodies targeting Ago2. After transfection with *miR-148a-5p* or *miR-148a-3p*, Ago2-bound miRNAs were isolated, and qRT-PCR was carried out to determine whether *miR-148a-5p* or *miR-148a-3p* was bound to Ago2 (Figure S2A,B).

After transfection of PANC-1 and SW1990 cells with *miR-148a-5p* and immunoprecipitation by anti-Ago2 antibodies, *miR-148a-5p* levels were significantly higher than those of mock or control transfected cells and those of *miR-148a-3p*-transfected cells (Figure S2C, middle). Similarly, after *miR-148a-3p* transfection, *miR-148a-3p* levels were significantly higher than those of mock or control transfected cells and those of *miR-148a-5p* transfected cells (Figure S2C, lower).

This suggests that *miR-148a-5p* was incorporated into RISC when *miR-148a-5p* was transfected, *miR-148a-3p* was incorporated into RISC when *miR-148a-3p* was transfected, and pre-*miR-148a* acts on cell lines separately to *miR-148a-5p* and *miR-148a-3p*. *miR-21* was used as an internal control of microRNA level expression between each sample (Figure S2C, upper).

3.3 | DNA methylation and *miR-148a* expression levels

Expression levels of *miR-148a-5p* and *miR-148a-3p* were markedly lower in the 2 cell lines (Figure 1A). To elucidate the molecular mechanisms underlying the low expression of *miR-148a-5p and miR-148a-3p* in PDAC cells, the PANC-1 cell line was treated with a demethylating agent (5-aza-2′-deoxycytidine [5-aza-dC]). Expression levels of *miR-148a-5p* and *miR-148a-3p* in PANC-1 cells were significantly elevated by 5-aza-dC treatment (Figure S3B). These data suggested that DNA methylation might cause silencing of *miR-148a-5p* and *miR-148a-3p* in PDAC cells.

3.4 | Effects of *miR-148a-5p* and *miR-148a-3p* expression on cell growth, apoptosis, migration and invasiveness of PDAC cell lines

Gain-of-function studies were carried out to investigate the functional roles of *miR-148a-5p* and *miR-148a-3p*. XTT assays showed significant inhibition of cell proliferation in PANC-1 or in SW1990 cells transfected with *miR-148a-5p* or *miR-148a-3p* in comparison with mock or control transfectants ($P < .0001$, Figure 1C). Apoptotic cell numbers (early apoptotic and late apoptotic cells) were significantly larger in *miR-148a-5p* or *miR-145-3p* transfectants than in mock or negative control transfectants (Figure S4A,B). Western blot analyses showed that cleaved PARP expression was significantly increased in *miR-148a-5p* or *miR-148a-3p* transfectants compared with mock or negative control transfectants (Figure S4C). In vitro assays showed that migration and invasion were significantly inhibited in *miR-148a-5p* or *miR-148a-3p* transfectants compared with mock or miR-control transfectants (each $P < .0001$, Figure 1D,E). These results suggested that pre-*miR-148a* could have an antitumor function in PDAC cells.

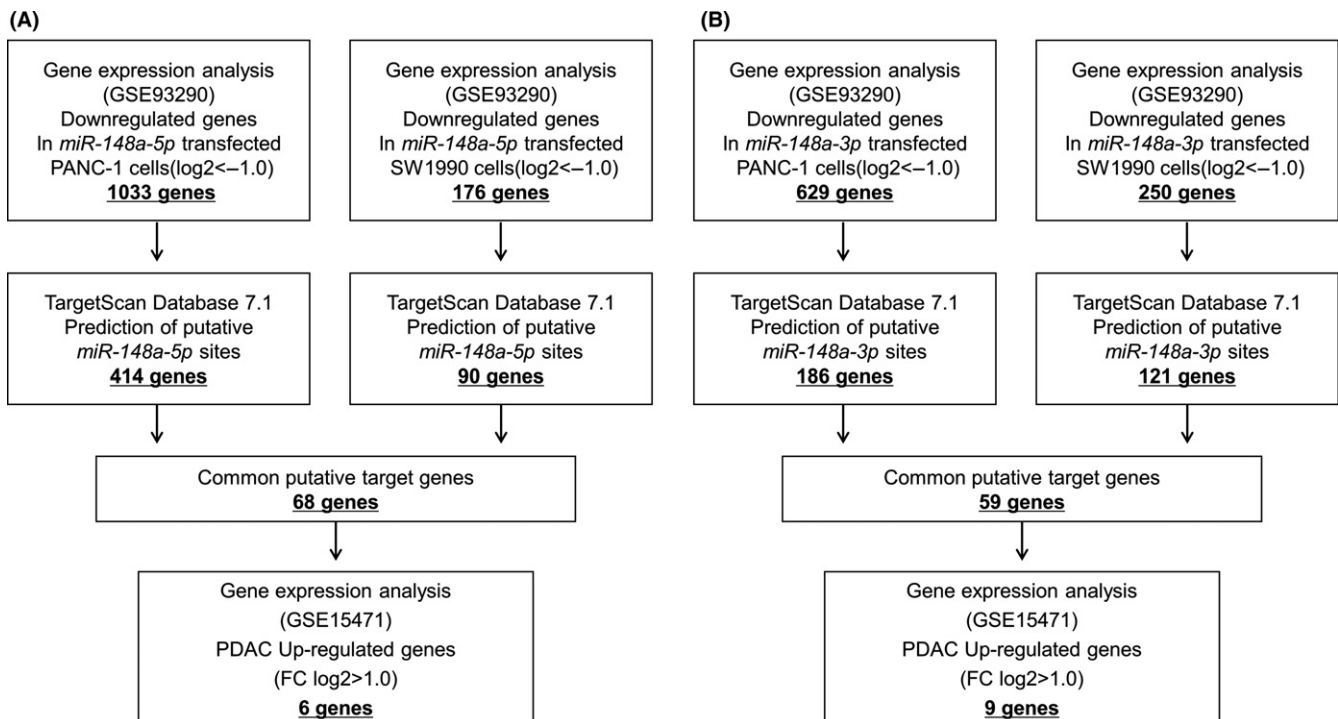## 3.5 | Identification of candidate genes regulated by *miR-148a-5p* and *miR-148-3p* in PDAC cells

Next, we attempted to identify target genes coordinately regulated by *miR-148-5p* and *miR-148a-3p*. The strategies for narrowing down the genes targeted by *miR-148a-5p and miR-148a-3p* are shown in Figure 2. We carried out a combination of in silico analysis, GEO

analysis and genome-wide gene expression analysis using PDAC cell lines (PANC-1 and SW1990) transfected with *miR-148a-5p* or *miR-148a-3p* (GEO accession number GSE93290).

In PANC-1 and SW1990 cells transfected with *miR-148a-5p*, a total of 1033 and 176 genes, respectively, were downregulated. Furthermore, the TargetScan database showed that 414 and 90 of those genes, respectively, had putative target sites for *miR-148a-5p* in their 3′-UTR. We found that there were 68 common genes targeted in both cell lines. Last, gene expression data showed that 6 of those genes were upregulated (fold-change $\log_2 > 1.0$) in cancer tissues according to GEO database analyses (GEO accession number GSE15471).

In *miR-148a-3p* transfectants, a total of 629 and 250 genes, respectively, were downregulated in PANC-1 and SW1990. Furthermore, the TargetScan database showed that 186 and 121 genes, respectively, had putative target sites for *miR-148a-3p* in their 3′-UTR. We found that there were 59 common genes targeted in both cell lines. Last, 9 genes were upregulated (fold-change $\log_2 > 1.0$) in cancer tissues by GEO database analyses (GEO accession number GSE15471).

We also checked the clinical significance of 6 genes targeted by *miR-148a-5p* (Table 3) and 9 genes targeted by *miR-148a-3p* (Table 4). Kaplan-Meier survival curves showed that high expression of all 6 of the genes was associated with poor prognoses in PDAC in the TCGA database. Target genes of *miR-148a-5p* included *PHLDA2*, *LPCAT2* and *AP1S3*, whereas target genes of *miR-148a-3p* included *SMS*, *ENDOD1* and *UHMK1* where mRNA expression levels were significantly upregulated. On TCGA database, patients showing elevated expression of all 6 target genes had a significantly poorer

FIGURE 2 Strategy for analysis of *pre-miR-148a* candidate target genes. Strategy for identification of putative candidate genes regulated by (A) *miR-148a-5p* and (B) *miR-148a-3p* in pancreatic ductal adenocarcinoma (PDAC) cells. Approach to identifying *miR-148a-5p* and *miR-148a-3p* target genes. We used in silico analysis of genome-wide gene expression, TargetScan and Gene Expression Omnibus (GEO) database analysis of *miR-148a-5p* and *miR-148a-3p* transfected PANC-1 and SW1990 cells

TABLE 3 Candidate target genes regulated by *miR-148a-5p*

Entrez gene ID	Gene symbol	Gene name	miR-148a-5p Target sites	Expression in miR-148a-5p transfectants FC(log$_2$)		GEO data (GSE15471) FC(log$_2$)	[a]TCGA_OncoLnc P-value
				PANC1	SW1990		
7262	PHLDA2	Pleckstrin homology-like domain, family A, member 2	1	−2.343	−1.560	2.847	.0361
11167	FSTL1	Follistatin-like 1	1	−1.307	−1.433	1.841	.2790
54947	LPCAT2	Lysophosphatidylcholine acyltransferase 2	4	−1.385	−1.458	1.474	.0039
23531	MMD	Monocyte to macrophage differentiation-associated	1	−1.816	−1.030	1.414	.6490
1808	DPYSL2	Dihydropyrimidinase-like 2	1	−2.039	−2.620	1.288	.9210
130340	AP1S3	Adaptor-related protein complex 1, sigma 3 subunit	2	−1.117	−1.313	1.166	.0041

GEO, Gene Expression Omnibus; TCGA, The Cancer Genome Atlas.
[a]Kaplan-Meier analysis log-rank *P*-value <.05, poor prognosis with a high expression.

TABLE 4 Candidate target genes regulated by *miR-148a-3p*

Entrez gene ID	Gene symbol	Gene name	miR-148a-3p Target sites	Expression in miR-148a-5p transfectants FC(log$_2$)		GEO data (GSE15471) FC(log$_2$)	[a]TCGA_OncoLnc P-value
				PANC1	SW1990		
3106	HLA-B	Major histocompatibility complex, class I, B	1	−1.333	−1.418	1.411	.7440
8829	NRP1	Neuropilin 1	2	−2.024	−1.411	1.302	.9850
6611	SMS	Spermine synthase	1	−1.447	−1.650	1.263	.0032
54492	NEURL1B	Neuralized homolog 1B (Drosophila)	1	−1.438	−1.528	1.236	.1540
3134	HLA-F	Major histocompatibility complex, class I, F	1	−1.401	−1.176	1.216	.2220
3105	HLA-A	Major histocompatibility complex, class I, A	2	−1.544	−1.713	1.187	.7310
23052	ENDOD1	Endonuclease domain containing 1	2	−1.135	−1.500	1.177	.0003
5476	CTSA	Cathepsin A	1	−1.747	−1.704	1.078	.2780
127933	UHMK1	U2AF homology motif (UHM) kinase 1	3	−1.583	−1.085	1.029	.0131

GEO, Gene Expression Omnibus; TCGA, The Cancer Genome Atlas.
[a]Kaplan-Meier analysis log-rank *P*-value <.05, poor prognosis with a high expression.

overall survival by Kaplan-Meier analysis (Figure 3). Furthermore, high expression of target genes tended to indicate recurrence and DFS was shorter (Figure 3). Next, we validated PDAC and normal pancreatic tissue in our specimens, and carried out qRT-PCR analysis of each target gene's mRNA expression level. *PHLDA2, LPCAT2, AP1S3, ENDOD1* and *UHMK1* showed significantly high expression in PDAC (Figure 4, left panels). In addition, we carried out qRT-PCR analysis of each target gene's mRNA expression level using RNA from PANC-1 and SW1990 cells that had been transfected with *miR-148a-5p* mimic or *miR-148a-3p* mimic. The data showed that each target gene's expression was downregulated (Figure 4, right panels).

In the present study, we focused on the Pleckstrin Homology Like Domain Family A Member 2 (*PHLDA2*) because *miR-148a-5p* (passenger strand) achieved the greatest degree of downregulation (Figure 4A, upper, right).

3.6 | Direct regulation of *PHLDA2* by *miR-148a-5p* in PDAC cells

Negative correlations were detected between *miR-148a-5p* and *PHLDA2* expression (*R* = −.495, *P* = .0007, Figure 5A). Both

PHLDA2 mRNA and PHLDA2 protein levels were markedly reduced in *miR-148a-5p* transfectant cells (Figure 4A, upper, right, Figure 5B).

The putative target site in the 3′-UTR of *PHLDA2* is shown in Figure S1. Luminescence intensity was significantly reduced by cotransfection with *miR-148a-5p* and the vector carrying the wild-type 3′-UTR (position 77-83), whereas transfection with the deletion vector (deletion of binding site) blocked the decrease in luminescence (*P* < .0001, Figure 5C).

A total of 30 specimens was evaluated by immunohistochemical staining. All tumors were of differentiated adenocarcinoma type (well, moderate and poor) and showed strong intracellular immunoreactivity. However, normal pancreatic tissue was not stained (Figure 5D).

3.7 | Effects of silencing *PHLDA2* on PDAC cell lines

To investigate the oncogenic functions of *PHLDA2* in PDAC cells by using si-*PHLDA2*, we evaluated the knockdown efficiency of si-*PHLDA2* transfection in PDAC cell lines. In this assay, we used 2 types of si-*PHLDA2* (si-*PHLDA2-1* and si-*PHLDA2-2*). Both siRNAs
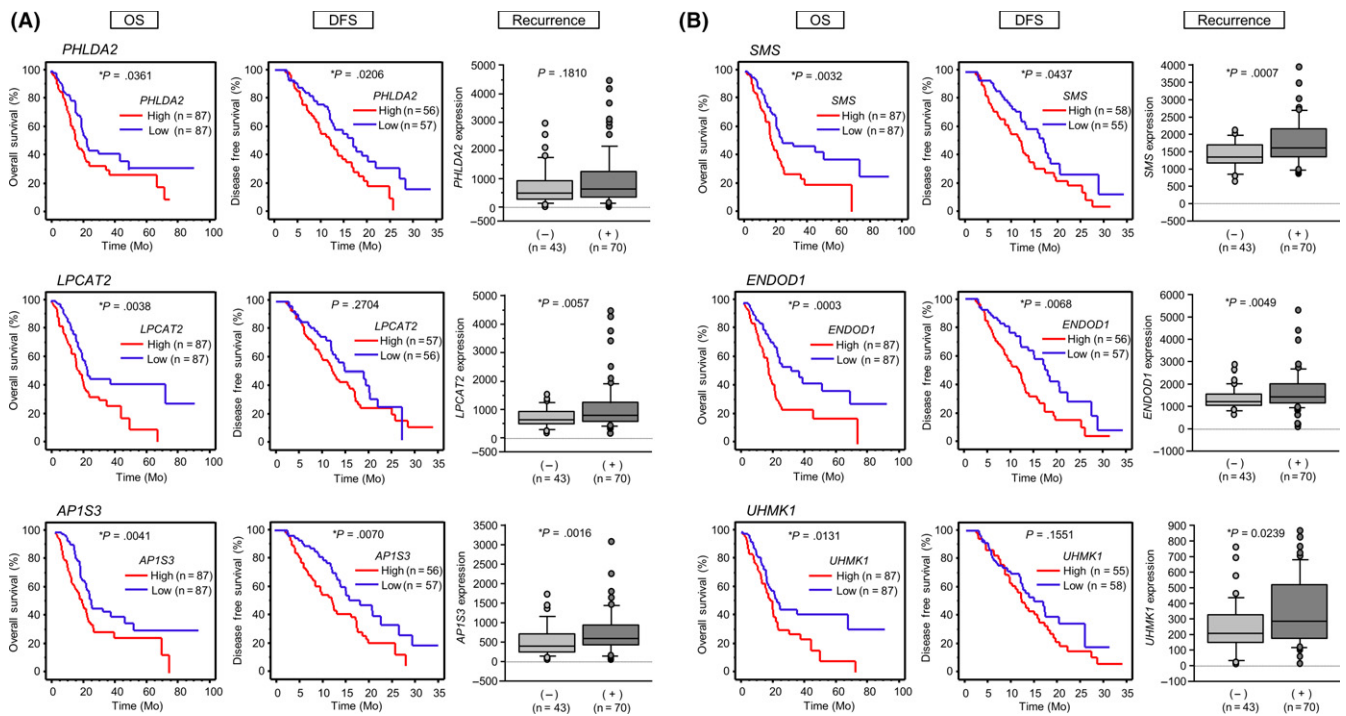
FIGURE 3 Overall survival, disease-free survival and recurrence of target genes by *miR-148a-5p* and *miR-148a-3p* on The Cancer Genome Atlas (TCGA) database. A, Three candidate genes modulated by *miR-148a-5p* (*PHLDA2*, *LPCAT2*, *AP1S3*). Kaplan-Meier analysis and the prognostic factors for pancreatic ductal adenocarcinoma (PDAC) are shown, *P < .05. B, Three candidate genes modulated by *miR-148a-3p* (*SMS*, *ENDOD1*, *UHMK1*). Kaplan-Meier analysis and the prognostic factors for PDAC are shown, *P < .05

effectively downregulated *PHLDA2* mRNA/PHLDA2 protein expression in both cell lines (*P* < .0001, Figure 6A,B).

Cancer cell proliferation, migration and invasion abilities were inhibited in si-*PHLDA2* transfectants compared with mock- or siRNA-control-transfected cells (Figure 6C-E). In the apoptosis assays, si-*PHLDA2*-1 and si-*PHLDA2*-2 transfection significantly increased apoptotic cells in PANC-1 cells (Figure S4A-C).

3.8 | Effects of cotransfection of *PHLDA2* and *miR-148a-5p* in PDAC cell lines

To confirm the antitumor effect of *miR-148a-5p*, we carried out rescue experiments using *PHLDA2* overexpression in PDAC cells with *miR-148a-5p* restoration. Rescue studies indicated that cancer cell migration and invasion properties were rescued by *PHLDA2* transfectants compared with cells with restored *miR-148a-5p* only (Figure 7). These data indicated that *PHLDA2* expression was regulated by *miR-148a-5p* and expression of *miR-148a-5p* induced antitumor effects on migration and invasion in PDAC cells.

## 3.9 | Investigation of downstream genes regulated by *PHLDA2* in PDAC cells

Our selection strategy of downstream genes regulated by *PHLDA2* is shown in Figure 8A. A total of 530 genes was commonly downregulated (log$_2$ ratio < −1.0) in si-*PHLDA2*-transfected PANC-1 cells. We also assessed the upregulated genes in PDAC tissues by GEO

database analyses (GEO accession number GSE15471). With that approach, we identified 37 genes (Table 5). Our microarray expression data were deposited in the GEO database (accession number GSE106791).

Furthermore, we checked the expression status of those genes and their pathological relations to PDAC by using TCGA-based large cohort study data. Kaplan-Meier analysis showed that PDAC patients with high expression of 12 genes (*SERPINA3*, *IFTM1*, *SDC1*, *FERMT1*, *CDK1*, *NEK2*, *MIXRA5*, *RRM2*, *ZWINT*, *ANLN*, *TOP2A* and *GJB2*) had significantly poorer overall survival (Figure 8B).

4 | DISCUSSION

Despite recent developments in treatment, advanced PDAC cannot be cured. Novel approaches for identification of therapeutic targets of PDAC are needed. Based on this, we have identified antitumor miRNAs that regulate cancer pathways in PDAC cells.[26] Our miRNA expression signature of PDAC showed that some passenger strands of miRNAs were significantly downregulated in PDAC.[8] We hypothesize that the data could help to identify miRNAs important for the development and progression of PDAC. In the present study, we focused on pre-*miR-148a* strands: *miR-148a-5p* (the passenger strand) and *miR-148a-3p* (the guide strand). With this focus, we investigated the functional significance of these specific miRNAs and regulatory RNA networks in PDAC cells.
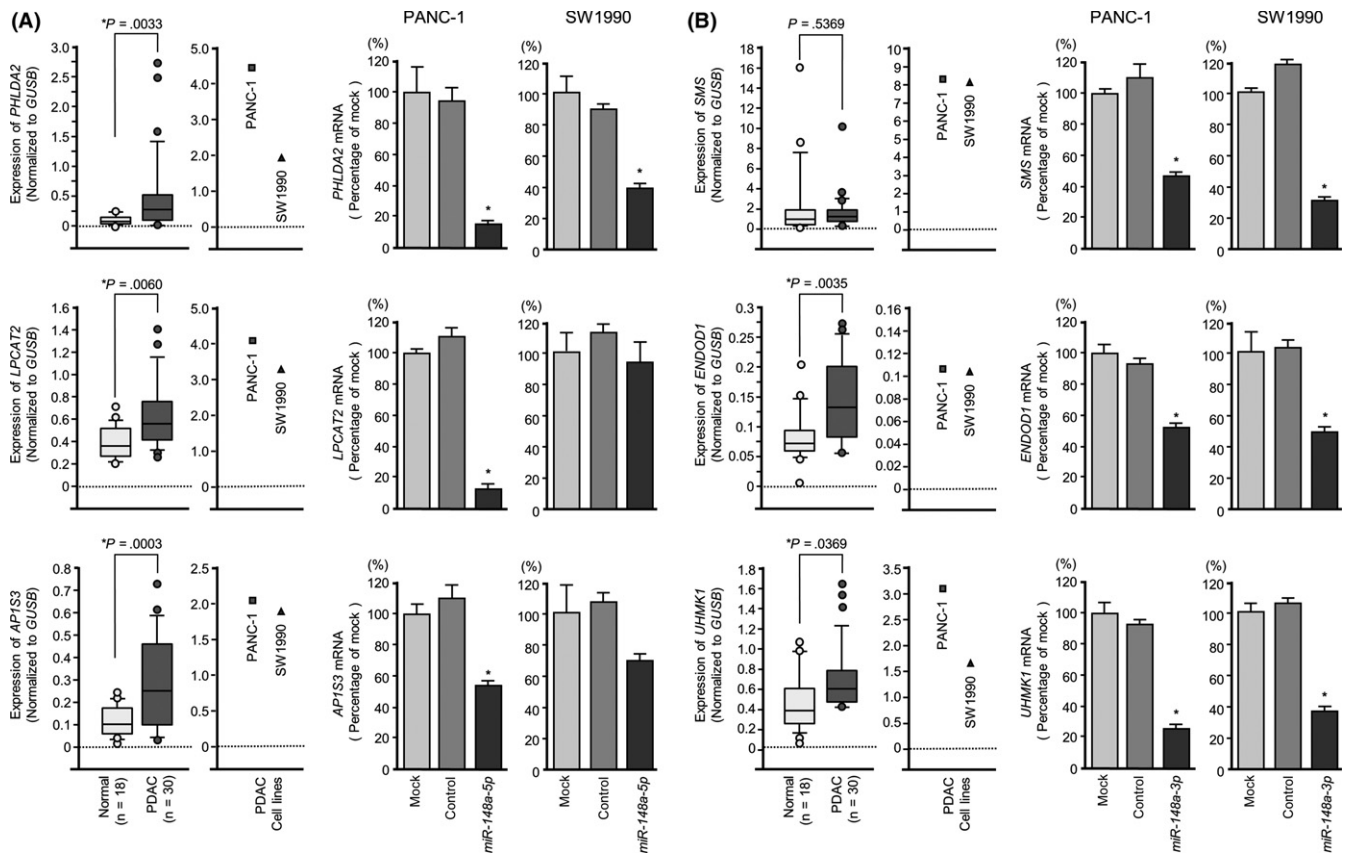
FIGURE 4 Messenger RNA expression of target genes of *miR-148a-5p* and *miR-148a-3p* on clinical sample and directly regulation of mRNA expression by *miR-148a-5p* and *miR-148a-3p* transfectants in pancreatic ductal adenocarcinoma (PDAC) cell lines. A, Expression levels of *miR-148a-5p* target genes (*PHLDA2*, *LPCAT2*, *AP1S3*) in PDAC clinical specimens and cell lines were determined by qRT-PCR. *GUSB* was used as an internal control, data were normalized to *GUSB* expression (left), *P < .05. Gene expression was directly downregulated by transfection of *miR-148a-5p* mimic (right), *P < .0001. B, Expression levels of *miR-148a-3p* target genes (*SMS*, *ENDOD1*, *UHMK1*) in PDAC clinical specimens and cell lines were determined by qRT-PCR. *GUSB* was used as an internal control, data were normalized to *GUSB* expression (left), *P < .05. Gene expression was directly downregulated by transfection of *miR-148a-3p* mimic (right), *P < .0001

In the human genome, the *miR-148*-family consists of 3 members that are located in different chromosomal regions: *miR-148a* is at 7p15.2, *miR-148b* is at 12q13.13 and *miR-152* is at 17q21.32.[27,28] The mature sequences of the guide strands of these miRNAs are similar and the seed sequences (UCAGUGCA) are identical.[29] Most analyses have focused on guide strands of the *miR-148*-family in normal physiological conditions or in cancer cells.[30,31] A large number of previous studies showed that *miR-148a-3p* (the guide strand) was downregulated in several types of cancer (eg, gastric cancer, colon cancer, hepatocellular carcinoma, breast cancer and PDAC).[32-36] The *miR-148a* gene contains a large number of CpG islands in the promoter (Figure S3A). In hepatocellular cancer, *miR-148a* is silenced by DNA hypermethylation.[37] In pancreatic cancer, a past study reported that aberrant hypermethylation of the *miR-148a* coding region progresses as pancreatic cancer malignancy increases.[38] We showed that hypermethylation suppresses *miR-148a-5p* and *miR-148a-3p* even in PDAC (Figure S3B). Our present study of *miR-148a-3p* is consistent with previous reports. A new finding of the present analysis was that *miR-148a-5p* (the passenger strand) acted as an antitumor miRNA as did *miR-148-3p* (the guide

strand) in PDAC cells. Involvement of the passenger strand of miRNA in cancer pathogenesis is a new concept in the field of miRNA research.

In the present study, we identified oncogenic genes regulated by *miR-148a-5p* and *miR-148a-3p* in PDAC cells by using genome-wide gene expression and miRNA database analyses. Three genes (*PHLDA2*, *LPCAT2* and *AP1S3*) were regulated by *miR-148a-5p* (passenger strand) and were identified as putative oncogenic genes in PDAC pathogenesis. Similarly, 3 genes (*SAS*, *ENDOD1* and *UHMK1*) were found to be regulated by *miR-148-3p* (the guide strand). Analysis of these genes will contribute to the elucidation of the molecular mechanism of PDAC pathogenesis.

We focused on *PHLDA2* and investigated its oncogenic functions because its expression in 2 pancreatic cancer cell lines showed the greatest suppression by *miR-148a-5p* (passenger strand). Moreover, the role of *PHLDA2* has been controversial in other carcinomas (ie, its roles as an "oncogene" or "tumor suppressor" are unclear).[39,40] Clinical features in TCGA database of PDAC patients showed there were no significant relationships in T, N, and M of TMN stage (data not shown). However, high expression of *PHLDA2* related to poor
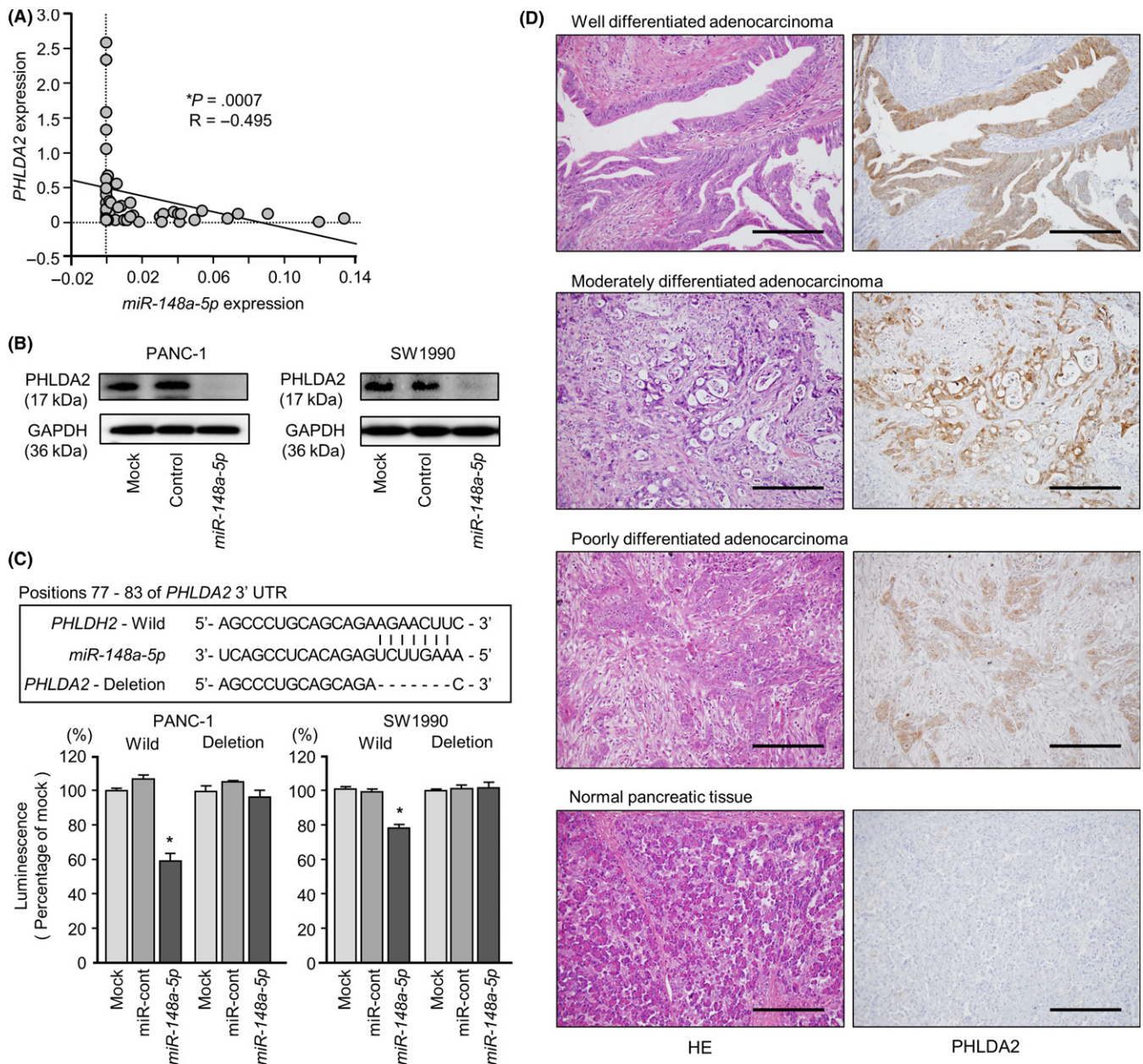
FIGURE 5 Direct regulation of *PHLDA2* by *miR-148a-5p* in pancreatic ductal adenocarcinoma (PDAC) cell lines and immunohistochemical staining of PHLDA2 protein in PDAC clinical specimens. A, Expression levels of *PHLDA2* and *miR-148a-5p* were negatively correlated. B, PHLDA2 protein expression in PDAC cell lines was evaluated by western blot analyses 96 h after transfection with *miR-148a-5p*. GAPDH was used as a loading control. C, *miR-148a-5p* binding sites in the 3′-UTR of *PHLDA2* mRNA. Dual luciferase reporter assays using vectors encoding the putative *miR-148a-5p* (positions 77-83) target site of the *PHLDA2* 3′-UTR for both wild-type and deleted regions. Normalized data were calculated as ratios of *Renilla*/firefly luciferase activities, *P < .05. D, Immunohistochemical staining of *PHLDA2* in PDAC specimens. All differentiated types of PDAC (well, moderate and poor) showed strong intracellular immunoreactivity (left panel, H&S staining; right panel, PHLDA2 staining; original magnification, ×200; scale bars, 200 μm)

OS and DFS. Past studies showed that *PHLDA2* acted as a growth-suppressive gene.[41] *PHLDA2* is located on human chromosome 11p15.5, a location known for imprinting gene clusters.[42] It is well known that dysregulation of this gene cluster is associated with Beckwith-Wiedemann syndrome.[43] To investigate the functional significance of *PHLDA2*, knockout mice or transgenic mouse studies have been carried out.[44] In *PHLDA2* null mice, placenta overgrowth

was observed and overexpression of *PHLDA2* resulted in placental stunting.[45] In humans, upregulation of *PHLDA2* was observed in intrauterine growth restriction placentas.[46] However, the relationship between *PHLDA2* expression and human cancers is not clear.

Our present study showed that *PHLDA2* was overexpressed in PDAC clinical specimens and that its expression enhanced cancer cell migration and invasion in PDAC cells. Moreover, high expression
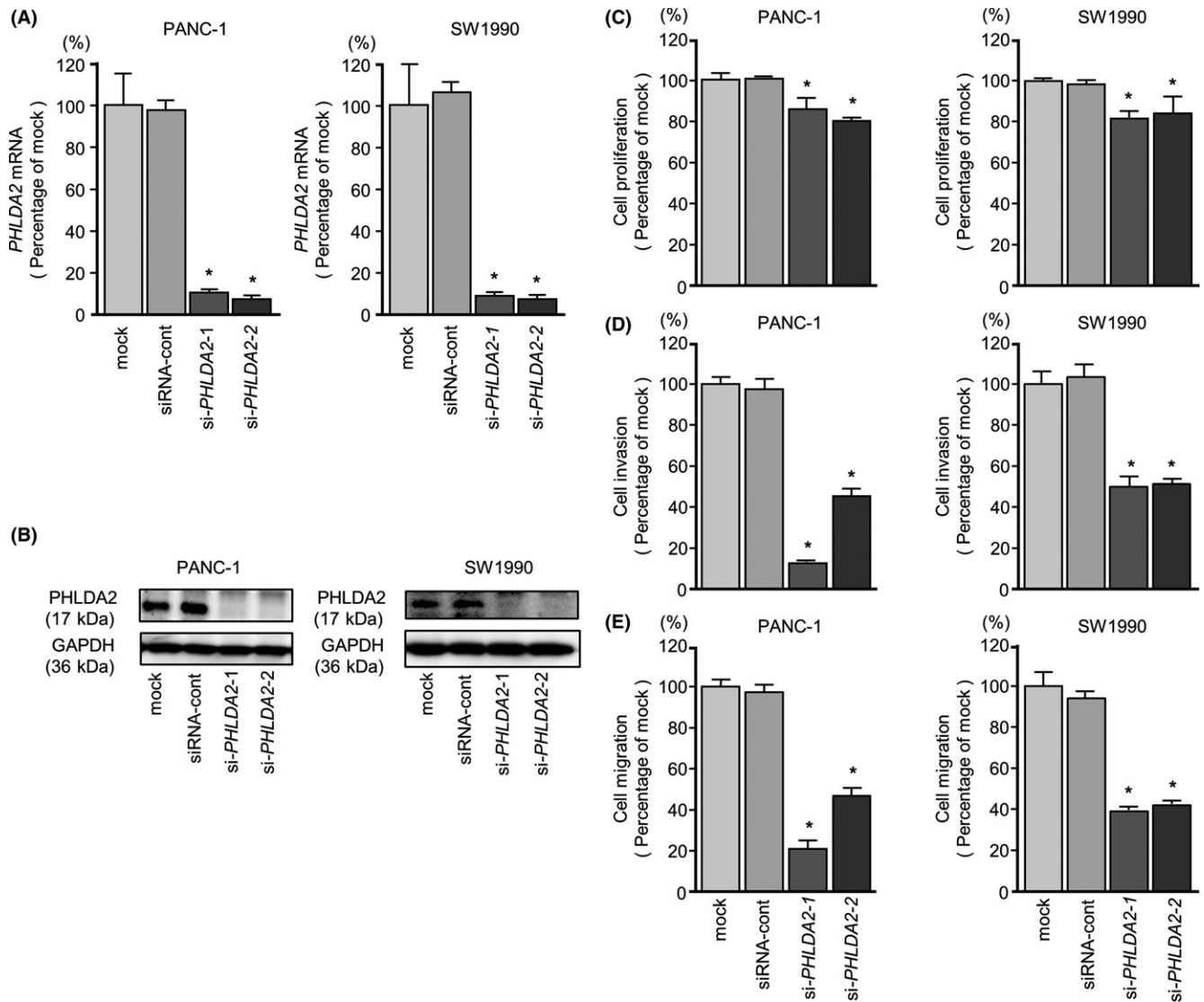
FIGURE 6 *PHLDA2* mRNA and PHLDA2 protein expression after *si-PHLDA2* transfection and the effects of *PHLDA2* knockdown in pancreatic ductal adenocarcinoma (PDAC) cell lines. A, *PHLDA2* mRNA expression in PDAC cell lines was evaluated by qRT-PCR 72 h after transfection with *si-PHLDA2*-1 or *si-PHLDA2*-2. *GUSB* was used as an internal control, data were normalized to *GUSB* expression. B, PHLDA2 protein expression in PDAC cell lines was evaluated by western blot analysis 96 h after transfection with *si-PHLDA2*-1 and *si-PHLDA2*-2. GAPDH was used as a loading control. C, Cell proliferation was determined with XTT assays 72 h after transfection with 10 nmol/L *si-PHLDA2*-1 or *si-PHLDA2*-2, *P < .0001. D, Cell invasion activity was determined using Matrigel invasion assays, *P < .0001. E, Cell migration activity was determined by migration assays, *P < .0001

of *PHLDA2* was significantly associated with poor prognosis of PDAC patients based upon a large cohort study. These findings indicate that aberrantly expressed *PHLDA2* acts like a cancer-promoting gene in PDAC cells. TCGA database analyses indicate that high expression of *PHLDA2* is significantly associated with poor prognoses in several types of cancer (eg, renal cell carcinoma, hepatocellular carcinoma and glioma). Functional analysis will be necessary to verify the cancer-promoting effects of *PHLDA2*.

Finally, we investigated genes mediated by *PHLDA2* in PDAC cells. Interestingly, past studies showed that aberrant expression of several of the genes (*SDC1, CDK1, ANLN* and *TOP2A*) contributes to cancer cell aggressiveness.[18,47-49] Among these genes, a total of 12 were deeply involved in PDAC pathogenesis by TCGA analyses. Our

data suggest that overexpression of *PHLDA2* might induce the expression of downstream cancer-promoting genes in PDAC cells. These results suggest that *PHLDA2* might be a possible therapeutic target for PDAC patients.

In conclusion, both strands of pre-*miR-148a* (*miR-148a-5p* and *miR-148a-3p*) were significantly reduced in PDAC clinical specimens. The passenger strand, *miR-148a-5p*, had a potent antitumor function through targeting of cancer-promoting genes in PDAC cells. *PHLDA2* was markedly elevated in PDAC, and it was involved in PDAC pathogenesis, suggesting *PHLDA2* could be used as a therapeutic target in PDAC. The involvement of passenger strand miRNAs in the regulation of cellular processes is a novel concept in RNA research.
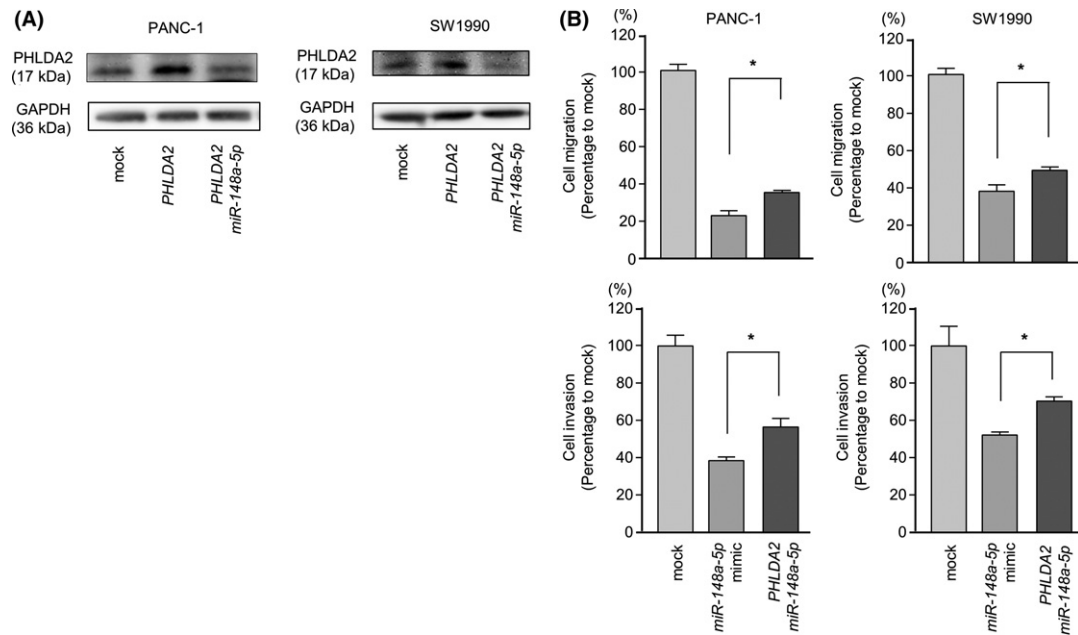
FIGURE 7 Rescue experiments: induction of *PHLDA2* overexpression in pancreatic ductal adenocarcinoma (PDAC) cell lines with *miR-148a-5p* restoration. A, PHLDA2 protein overexpression in PANC-1 and SW1990 was evaluated by western blot analyses 72 h after 0.5 μg/well transfection with *PHLDA2* cDNA plasmid (middle bands). PHLDA2 protein overexpression was attenuated 72 h after cotransfection with 0.5 μg/well *PHLDA2* cDNA plasmid and 10 nmol/L *miR-148a-5p* mimic (right bands). GAPDH was used as a loading control. B, Cell migration activity was assessed 72 h after cotransfection with 0.5 μg/well *PHLDA2* cDNA plasmid and 10 nmol/L *miR-148a-5p* mimic, $*P < .0001$. Cell invasion activity was determined using Matrigel invasion assays 72 h after cotransfection with 0.5 μg/well *PHLDA2* cDNA plasmid and 10 nmol/L *miR-148a-5p* mimic, $*P < .0001$
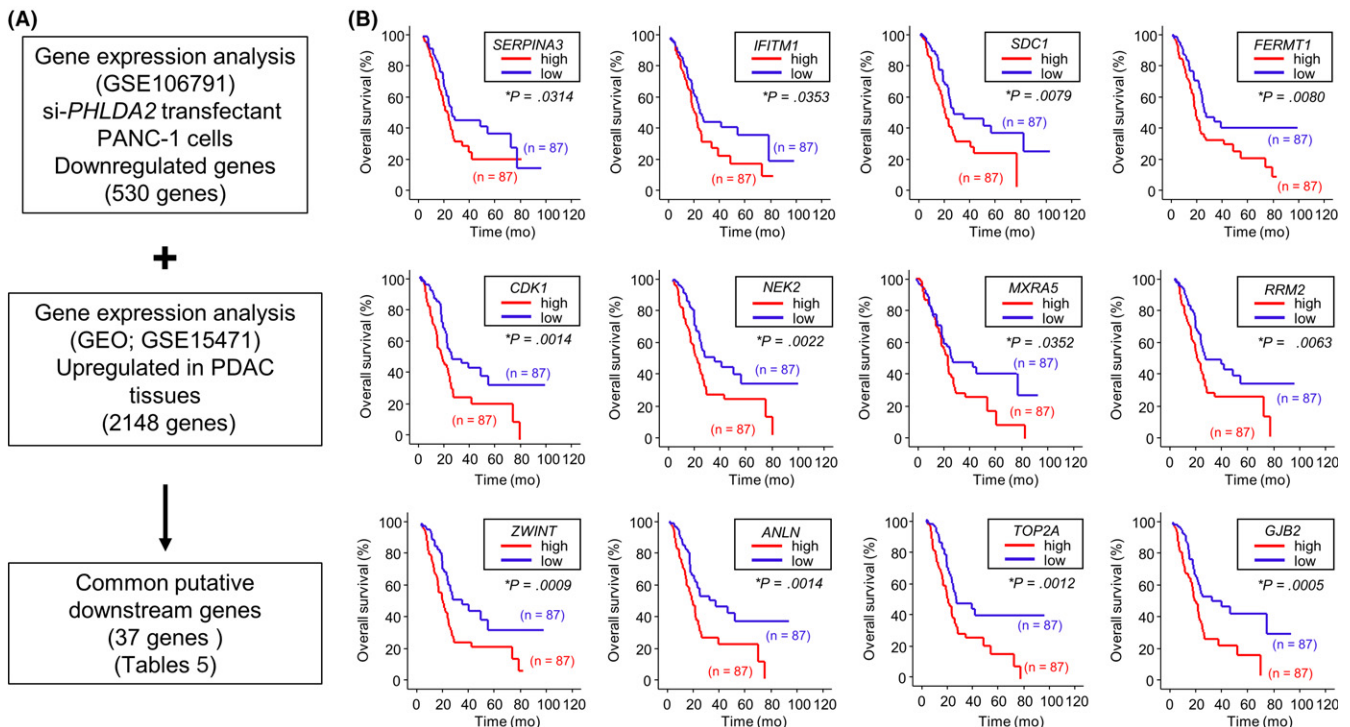
FIGURE 8 Strategy for analysis of *PHLDA2* downstream genes. A, Flow chart illustrates the strategy for analysis of *PHLDA2*-mediated downstream genes in pancreatic ductal adenocarcinoma (PDAC) cells. B, Kaplan–Meier plots of overall survival with log-rank tests between those with high and low expression of 12 genes downstream from *PHLDA2* in the PDAC Cancer Genome Atlas (TCGA) database. GEO, Gene Expression Omnibus

TABLE 5 Downregulated genes by *si-PHLDA2* transfectants

Entrez gene ID	Gene symbol	Gene name	Mock vs si-PHLDA2_2 logFC	GEO logFC	OncoLnc P-value
12	SERPINA3	Serpin peptidase inhibitor, clade A (alpha-1 antiproteinase, antitrypsin), member 3	−2.4052	1.1210	**.0314**
115207	KCTD12	Potassium channel tetramerization domain containing 12	−1.7676	1.2730	.0245
25924	MYRIP	Myosin VIIA and Rab interacting protein	−1.7485	1.4215	.099
8519	IFITM1	Interferon induced transmembrane protein 1	−1.5832	1.4437	**.0353**
23621	BACE1	Beta-site APP-cleaving enzyme 1	−1.5579	1.6490	.31
6382	SDC1	Syndecan 1	−1.5511	1.3845	**.00787**
5738	PTGFRN	Prostaglandin F2 receptor inhibitor	−1.4976	1.4021	.35
56605	ERO1LB	ERO1-like beta (S. cerevisiae)	−1.4052	1.6621	No data
92241	RCSD1	RCSD domain containing 1	−1.3758	1.1930	.569
23075	SWAP70	SWAP switching B-cell complex 70 kDa subunit	−1.3742	1.0542	.51
55612	FERMT1	Fermitin family member 1	−1.3590	1.6579	**.00799**
3613	IMPA2	Inositol(myo)-1(or 4)-monophosphatase 2	−1.3188	1.5101	.615
57619	SHROOM3	Shroom family member 3	−1.3051	1.1286	.132
2494	NR5A2	Nuclear receptor subfamily 5, group A, member 2	−1.2469	1.5494	.209
983	CDK1	Cyclin-dependent kinase 1	−1.2366	1.4143	**.00137**
54492	NEURL1B	Neuralized E3 ubiquitin protein ligase 1B	−1.2230	1.2359	.154
11037	STON1	Stonin 1	−1.2048	1.5983	.654
10403	NDC80	NDC80 kinetochore complex component	−1.1913	1.5473	.126
253827	MSRB3	Methionine sulfoxide reductase B3	−1.1684	1.8859	.902
4751	NEK2	NIMA-related kinase 2	−1.1547	1.0279	**.0022**
25878	MXRA5	Matrix-remodeling associated 5	−1.1433	2.3870	**.0352**
285590	SH3PXD2B	SH3 and PX domains 2B	−1.1361	1.3111	.848
84168	ANTXR1	Anthrax toxin receptor 1	−1.1311	2.9025	.28
51316	PLAC8	Placenta-specific 8	−1.1274	1.6964	.0588
6241	RRM2	Ribonucleotide reductase M2	−1.1057	1.1664	**.00627**
11130	ZWINT	ZW10 interacting kinetochore protein	−1.1000	1.1604	**.000948**
1728	NQO1	NAD(P)H dehydrogenase, quinone 1	−1.0986	2.1867	.61
54443	ANLN	Anillin, actin binding protein	−1.0854	1.7292	**.00142**
56925	LXN	Latexin	−1.0769	2.0471	.964
7153	TOP2A	Topoisomerase (DNA) II alpha 170 kDa	−1.0455	1.5302	**.0012**
4085	MAD2L1	MAD2 mitotic arrest deficient-like 1 (yeast)	−1.0324	1.1864	.108
2706	GJB2	Gap junction protein, beta 2, 26 kDa	−1.0296	3.6935	**.000459**
1999	ELF3	E74-like factor 3 (ets domain transcription factor, epithelial-specific)	−1.0295	1.1854	.174
9891	NUAK1	NUAK family, SNF1-like kinase, 1	−1.0212	1.6399	.827
4016	LOXL1	Lysyl oxidase-like 1	−1.0207	2.3387	.778
1786	DNMT1	DNA (cytosine-5)-methyltransferase 1	−1.0184	1.2180	.117
3223	HOXC6	Homeobox C6	−1.0145	1.9164	.391

Bold values, Kaplan-Meier analysis log-rank *P*-value <.05, poor prognosis with a high expression.
Italic value, Kaplan-Meier analysis log-rank *P*-value <.05, poor prognosis with a low expression.
GEO, Gene Expression Omnibus; PDAC, pancreatic ductal adenocarcinoma.

CONFLICT OF INTEREST

Authors declare no conflicts of interest for this article.

ORCID

Tetsuya Idichi (iD) http://orcid.org/0000-0001-8048-2203
Hiroshi Kurahara (iD) http://orcid.org/0000-0002-7735-9607

REFERENCES

1. Kamisawa T, Wood LD, Itoi T, Takaori K. Pancreatic cancer. *Lancet*. 2016;388:73-85.
2. Gillen S, Schuster T, Meyer Zum Buschenfelde C, Friess H, Kleeff J. Preoperative/neoadjuvant therapy in pancreatic cancer: a systematic review and meta-analysis of response and resection percentages. *PLoS Med*. 2010;7:e1000267.
3. Chrystoja CC, Diamandis EP, Brand R, Ruckert F, Haun R, Molina R. Pancreatic cancer. *Clin Chem*. 2013;59:41-46.
4. Bartel DP. MicroRNAs: target recognition and regulatory functions. *Cell*. 2009;136:215-233.
5. Zhang Y, Wang Z, Gemeinhart RA. Progress in microRNA delivery. *J Control Release*. 2013;172:962-974.
6. Fukumoto I, Hanazawa T, Kinoshita T, et al. MicroRNA expression signature of oral squamous cell carcinoma: functional role of microRNA-26a/b in the modulation of novel cancer pathways. *Br J Cancer*. 2015;112:891-900.
7. Fuse M, Kojima S, Enokida H, et al. Tumor suppressive microRNAs (miR-222 and miR-31) regulate molecular pathways based on microRNA expression signature in prostate cancer. *J Hum Genet*. 2012;57:691-699.
8. Yonemori K, Seki N, Idichi T, et al. The microRNA expression signature of pancreatic ductal adenocarcinoma by RNA sequencing: antitumour functions of the microRNA-216 cluster. *Oncotarget*. 2017;8:70097-70115.
9. Gregory RI, Chendrimada TP, Cooch N, Shiekhattar R. Human RISC couples microRNA biogenesis and posttranscriptional gene silencing. *Cell*. 2005;123:631-640.
10. Hutvagner G, Zamore PD. A microRNA in a multiple-turnover RNAi enzyme complex. *Science*. 2002;297:2056-2060.
11. Matranga C, Tomari Y, Shin C, Bartel DP, Zamore PD. Passenger-strand cleavage facilitates assembly of siRNA into Ago2-containing RNAi enzyme complexes. *Cell*. 2005;123:607-620.
12. Koshizuka K, Hanazawa T, Kikkawa N, et al. Regulation of ITGA3 by the anti-tumor miR-199 family inhibits cancer cell migration and invasion in head and neck cancer. *Cancer Sci*. 2017;108:1681-1692.
13. Osako Y, Seki N, Koshizuka K, et al. Regulation of SPOCK1 by dual strands of pre-miR-150 inhibit cancer cell migration and invasion in esophageal squamous cell carcinoma. *J Hum Genet*. 2017;62:935-944.
14. Goto Y, Kurozumi A, Arai T, et al. Impact of novel miR-145-3p regulatory networks on survival in patients with castration-resistant prostate cancer. *Br J Cancer*. 2017;117:409-420.
15. Mataki H, Seki N, Mizuno K, et al. Dual-strand tumor-suppressor microRNA-145 (miR-145-5p and miR-145-3p) coordinately targeted MTDH in lung squamous cell carcinoma. *Oncotarget*. 2016;7:72084-72098.
16. Matsushita R, Yoshino H, Enokida H, et al. Regulation of UHRF1 by dual-strand tumor-suppressor microRNA-145 (miR-145-5p and miR-145-3p): inhibition of bladder cancer cell aggressiveness. *Oncotarget*. 2016;7:28460-28487.
17. Sobin LH, Gospodarowicz MK, Wittekind C, eds. *TNM Classification of Malignant Tumours*, 7th edn. Chichester, UK: Wiley-Blackwell; 2010.
18. Idichi T, Seki N, Kurahara H, et al. Regulation of actin-binding protein ANLN by antitumor miR-217 inhibits cancer cell aggressiveness in pancreatic ductal adenocarcinoma. *Oncotarget*. 2017;8:53180-53193.
19. Yonemori K, Seki N, Kurahara H, et al. ZFP36L2 promotes cancer cell aggressiveness and is regulated by antitumor microRNA-375 in pancreatic ductal adenocarcinoma. *Cancer Sci*. 2017;108:124-135.
20. Kinoshita T, Nohata N, Hanazawa T, et al. Tumour-suppressive microRNA-29s inhibit cancer cell migration and invasion by targeting laminin-integrin signalling in head and neck squamous cell carcinoma. *Br J Cancer*. 2013;109:2636-2645.
21. Miyamoto K, Seki N, Matsushita R, et al. Tumour-suppressive miRNA-26a-5p and miR-26b-5p inhibit cell aggressiveness by regulating PLOD2 in bladder cancer. *Br J Cancer*. 2016;115:354-363.
22. Ichimi T, Enokida H, Okuno Y, et al. Identification of novel microRNA targets based on microRNA signatures in bladder cancer. *Int J Cancer*. 2009;125:345-352.
23. Osako Y, Seki N, Kita Y, et al. Regulation of MMP13 by antitumor microRNA-375 markedly inhibits cancer cell migration and invasion in esophageal squamous cell carcinoma. *Int J Oncol*. 2016;49:2255-2264.
24. Anaya J. OncoLnc: linking TCGA survival data to mRNAs, miRNAs, and lncRNAs. *PeerJ Comput Sci*. 2016;2:e67.
25. Anaya J. OncoRank: a pan-cancer method of combining survival correlations and its application to mRNAs, miRNAs, and lncRNAs. *PeerJ Prepr*. 2016;1:e2574.
26. Yonemori K, Kurahara H, Maemura K, Natsugoe S. MicroRNA in pancreatic cancer. *J Hum Genet*. 2017;62:33-40.
27. Chen X, Wang G, Lu X, et al. Polymorphisms and haplotypes of the miR-148/152 family are associated with the risk and clinicopathological features of gastric cancer in a Northern Chinese population. *Mutagenesis*. 2014;29:401-407.
28. Friedrich M, Pracht K, Mashreghi MF, Jack HM, Radbruch A, Seliger B. The role of the miR-148/-152 family in physiology and disease. *Eur J Immunol*. 2017;47:2026-2038.
29. Chen Y, Song YX, Wang ZN. The microRNA-148/152 family: multifaceted players. *Mol Cancer*. 2013;12:43.
30. Li Y, Deng X, Zeng X, Peng X. The role of Mir-148a in cancer. *J Cancer*. 2016;7:1233-1241.
31. Miao C, Zhang J, Zhao K, et al. The significance of microRNA-148/152 family as a prognostic factor in multiple human malignancies: a meta-analysis. *Oncotarget*. 2017;8:43344-43355.
32. Xia J, Guo X, Yan J, Deng K. The role of miR-148a in gastric cancer. *J Cancer Res Clin Oncol*. 2014;140:1451-1456.
33. Takahashi M, Cuatrecasas M, Balaguer F, et al. The clinical significance of MiR-148a as a predictive biomarker in patients with advanced colorectal cancer. *PLoS ONE*. 2012;7:e46684.
34. Pan L, Huang S, He R, Rong M, Dang Y, Chen G. Decreased expression and clinical significance of miR-148a in hepatocellular carcinoma tissues. *Eur J Med Res*. 2014;19:68.
35. Xu X, Zhang Y, Jasper J, et al. MiR-148a functions to suppress metastasis and serves as a prognostic indicator in triple-negative breast cancer. *Oncotarget*. 2016;7:20381-20394.
36. Feng H, Wang Y, Su J, et al. MicroRNA-148a suppresses the proliferation and migration of pancreatic cancer cells by down-regulating ErbB3. *Pancreas*. 2016;45:1263-1271.
37. Long XR, He Y, Huang C, Li J. MicroRNA-148a is silenced by hypermethylation and interacts with DNA methyltransferase 1 in hepatocellular carcinogenesis. *Int J Oncol*. 2014;44:1915-1922.
38. Hanoun N, Delpu Y, Suriawinata AA, et al. The silencing of microRNA 148a production by DNA hypermethylation is an early event in pancreatic carcinogenesis. *Clin Chem*. 2010;56:1107-1118.
39. Moon HG, Oh K, Lee J, et al. Prognostic and functional importance of the engraftment-associated genes in the patient-derived xenograft models of triple-negative breast cancers. *Breast Cancer Res Treat*. 2015;154:13-22.

40. Wang X, Li G, Koul S, et al. PHLDA2 is a key oncogene-induced negative feedback inhibitor of EGFR/ErbB2 signaling via interference with AKT signaling. *Oncotarget*. 2018;9:24914-24926.

41. Jensen AB, Tunster SJ, John RM. The significance of elevated placental PHLDA2 in human growth restricted pregnancies. *Placenta*. 2014;35:528-532.

42. Smith AC, Choufani S, Ferreira JC, Weksberg R. Growth regulation, imprinted genes, and chromosome 11p15.5. *Pediatr Res*. 2007;61:43R-47R.

43. Choufani S, Shuman C, Weksberg R. Molecular findings in Beckwith-Wiedemann syndrome. *Am J Med Genet* 2013;163c:131-140.

44. Frank D, Fortino W, Clark L, et al. Placental overgrowth in mice lacking the imprinted gene Ipl. *Proc Natl Acad Sci USA*. 2002;99:7490-7495.

45. Salas M, John R, Saxena A, et al. Placental growth retardation due to loss of imprinting of Phlda2. *Mech Dev*. 2004;121:1199-1210.

46. Cordeiro A, Neto AP, Carvalho F, Ramalho C, Doria S. Relevance of genomic imprinting in intrauterine human growth expression of CDKN1C, H19, IGF2, KCNQ1 and PHLDA2 imprinted genes. *J Assist Reprod Genet*. 2014;31:1361-1368.

47. Inki P, Jalkanen M. The role of syndecan-1 in malignancies. *Ann Med*. 1996;28:63-67.

48. Gan W, Zhao H, Li T, Liu K, Huang J. CDK1 interacts with iASPP to regulate colorectal cancer cell proliferation through p53 pathway. *Oncotarget*. 2017;8:71618-71629.

49. Pei YF, Yin XM, Liu XQ. TOP2A induces malignant character of pancreatic cancer through activating beta-catenin signaling pathway. *Biochim Biophys Acta*. 2017;1864:197-207.

SUPPORTING INFORMATION

Additional Supporting Information may be found online in the supporting information tab for this article.